APPLICATION OF RAMAN DIAGNOSTICS TO COMBUSTION

FINAL REPORT

April 1980

Principal Investigator: Lederman

Prepared For

NATIONAL AERONAUTICS AND SPACE ADMINISTRATION

NASA Lewis Research Center

Cleveland, Ohio

Grant No. NSG 3108

POLYTECHNIC INSTITUTE OF NEW YORK

AERODYNAMICS LABORATORIES

POLY M/AE Report No. 80-8

THE APPLICATION OF RAMAN DIAGNOSTICS TO COMBUSTION

by,

C. Posillico, A. Celentano, and S. Lederman

Introduction

The main purpose of this grant was essentially to provide support for a graduate student who was interested in diagnostics of combustion as a major part of his Ph.D thesis. This goal has been accomplished. Mr. Anthony Celentano is now completing his thesis and will be graduating soon. This grant provided, in addition, the opportunity for a masters degree candidate to familiarize himself with some aspects of combustion diagnostics. As far as the technical aspects of internal high pressure combustion diagnostics are concerned, a number of difficulties developed in the course of this work. Those difficulties and some results will be discussed in what follows.

The Diagnostic System

Due to the fundamental advantages presented by the Raman scattering techniques which have been discussed at great length in the literature, an attempt has been made to utilize these in this work. It must be pointed out that the Raman diagnostic technique has been pioneered and utilized in this laboratory for a number of years as can be seen from the Reference.

The transferal of the technique to internal combustion systems appeared to be a trivial matter. As it turned out the access ports, the combustion products and the geometry of the system combined to make this a very difficult problem.

In any case, the Raman diagnostic system was chosen primarily for the well known properties of the diagnostic techniques, which is apparent partially from the basic working equations:

$$I_{sA} = CNI_o(\nu_o \pm \nu)^4 \, [1-\exp(-hc\nu/kT)]^{-1} \qquad (1)$$

and

$$T = \frac{h\nu c}{k} \left[\ln \frac{I_s}{I_{as}} + 4 \ln \left(\frac{\nu_o+\nu}{\nu_o-\nu}\right)\right]^{-1} \qquad (2)$$

Thus the specie concentrations and their temperatures can be determined simultaneously, instantaneously and remotely. Since the Raman signals are independently and simultaneously measurable, there is no limit to the number of species that can be distinguished in a mixture of species as long as the specific vibrational frequencies of the species involved are resolvable by the equipment available.

The basic diagnostic arrangement is shown in Fig. 1. The number of the receiving stations is only limited by the number of available photomultiplier tubes, power supplies and data acquisition channels. A photographic view of the diagnostic system is shown in Fig. 2.

The Experimental Apparatus

As mentioned previously, one of the goals of this program was the development of a laser based diagnostic system for high pressure internal combustion. Due to a number of considerations such as laboratory space and location (enclosed laboratory without proper ventilation), it was decided to utilize methane as the principal fuel in a self-contained high pressure combustor. In this system shown in Fig. 3 the fuel and oxidant could be mixed to any desired concentration and to any given pressure beforehand. Therefore, the "fuel rich" and "fuel lean" mixtures can easily be attained as well as the stoichiometric mixtures. In this chamber various blends of fuels and different oxidants may also be inserted for analysis. Further, once the combustion has taken place,

the by-products may be held indefinitely for continued analysis. Due to the size of the access ports (1/2D) only one specie at a time could be monitored in the present combustion configuration. Therefore N_2 which is relatively stable in the combustion process was supposed to be used to obtain temperature information during the combustion process. To that end, the intensity of the Raman Stokes and the Raman anti-Stokes radiation were supposed to be recorded using two photomultiplier tubes focussed at the same point in the combustion chamber. The ratio of the scattered intensities would provide the temperature according to equation 2.

As is evident from the schematic diagram of the diagnostic apparatus, Fig. 1, the laser utilized in this work was a Q-switched ruby laser (6943Å) of approximately 2.5 joule laser energy at a pulse duration of approximately 20 nsec. This results in a laser pulse of 125 megawatt peak power. The Stokes line of N_2 at 8283Å and the anti-Stokes line at 5976Å were to be collected by 2 separate photomultipliers which were equipped with proper focussing lenses and narrow bandpass filters corresponding to the desired radiations and, in addition, to bandstop filters centered at 6943Å to eliminate Rayleigh and the radiation from the signals.

Experimental Procedure

The dimensions of the cylindrical combustor are given in Figure 3. The main problem concerning this particular experimental set up is being able to have the ruby laser pass through the combustor at the desired time during the interval of combustion. Therefore, some sort of triggering circuit based upon the time of the combustion is needed. At first an impulse from the ignition circuit which initiated the combustion was used to trip the laser

control panel which can be armed to fire and await a tripping pulse. However, there were several problems with this method. Due to the high voltage inherent in the ignition system a severe amount of electrical noise was generated by coupling the triggering system to the laser control panel. Further, and a more crucial problem than electrical noise was the fact that the combustion itself turned out to be independent of the initiating spark impulse. That is, the combustion could be only initiated at a desired time, but the time of maximum heat release from the point of initiation was variant for each successive separate combustion. This occurred despite the fact that measured amounts of methane and air were charged into the combustor for each sample. The reasons for the variable time of maximum heat release contain many factors, two major ones being internal mixing and temperature increase of the combustor after each successive explosion. There is virtually no means to control these factors. As a result, since the laser would be tripped invariantly with each ignition impulse, the actual laser beam fired at different times during the combustion process for each sample, giving unrelated sets of data.

A more satisfactory method was needed to trip the laser. Many methods were tried but the most successful proved to be using a photodiode set in front of a small viewing window directly in the chamber wall. Now the system could be so arranged as to trip the laser at the maximum output signal of the diode (i.e.: at the maximum light and heat output of the combustion process) completely independent of when the mixture was ignited or how long combustion lasted (see Fig. 4).

Several advantages were also gained by using the system shown in Figure 4. Firstly, since a photodiode was being used to trip the system, by monitoring the complete output of the photodiode during the combustion process on a storage oscilloscope, one could maintain a record of the relative intensity as well as the duration of the combustion indirectly through the total light output of the explosion.

Another advantage of the given system in Fig. 4 is that using the photodiode signal to trip an oscilloscope with a variable delayed output signal (as shown in diagram), then using that signal to tip the laser, one can "sweep" through the combustion process by varying the delayed signal from the oscilloscope and monitoring it against the photodiode signal.

The laser photodiode shown in Fig. 4 is used to monitor laser energy and arm the oscilloscope shown to receive signals from the phototubes. An iris is used to narrow the laser beam to prevent scattering inside the stainless steel combustor; a lens is used to focus down the laser beam into the combustor in order to strengthen the Raman signals.

Experimental Results

As mentioned in the previous section, it was possible to delay the firing of the laser to any desired time during the combustion. A delay of about 140 ms. fired the laser at the maximum heat release of the combustion. However, in Fig. 5, as a reference, are shown readings of the combustor evacuated (background reading) and the Raman Stokes signal of methane and air before ignition, which are well above the background, due mostly to scattering and reflections off the chamber walls of the primary beam.

In Figure 6, the photograph on the right has two traces: the one on top shows the evolution of the combustion in terms of the photodiode (at the combustor) output. The bottom trace shows where the varying delay pulse to fire the laser is set. By moving this pulse anywhere along the horizontal trace, the laser can be fired at any time during the explosion. However, even with zero delay, the earliest the trigger pulse can arrive at the laser is 100 ms. due to inherent internal delays in the entire system. This is the case in Fig. 6. Note, however, from the photodiode trace, that even at 100 ms. delay, the combustion has barely developed. Therefore, this would be a good place to start a "sweep" through the combustion by varying the trigger pulse to the laser for each combustion cycle. Note the difference in profile in the photodiode trace in Fig. 6 and in subsequent traces in Fig. 7 for example. This is due to the aforementioned variance of completion of combustion in each case.

Most importantly, however, is the lack of a noticeable Raman Stokes signal in the left-hand photographs in Figs. 6 and 7. Theory predicts the decrease of the Stokes signal during combustion but not the absence of one. Also note there is no discernable change in the zero signal reading during most of the Raman Stokes "sweep" until Fig. 8 at which point most of the combustion has taken place. Here, the sweep seems to be recovering some type of signal which grows as the combustion dies out. This is shown in Fig. 9, where a number of signals have been superimposed corresponding to varying delays after the combustion peak. The same process has been followed in the case of anti-Stokes lines with the same results.

Conclusion

The unexpected data obtained during this experiment were very confusing and many suggestions were formed as to the possible causes.

After a process of elimination of a number of suggestions, finally one emerged which could not be totally disapproved: the water vapor formed as a by-product of combustion apparently was absorbing the ruby laser line (6943Å) before it could even effect a Raman shift in nitrogen. Even the background signals or reflections and scattering effects of the combustor interior were also being absorbed by the water vapor. Therefore, a complete zero signal was being obtained.

Besides the scattering effect of the water droplets, the light coming from the combustion itself which was mentioned briefly before can also be a source of trouble. Noting Fig. 10, we see that the combustion light spectrum does not appear to be particularly intense except in the infrared region (around 7000Å). These particular photographs were taken with Tracor Northern's intensified diode array detector system. From Fig. 10 we see that at 8283Å (N_2 Stokes line) the intensity corresponds to 8689 "counts", compared to 21554 "counts" at the 7132Å line (which is to be expected in a hot combustion).

Now recalling the Raman N_2 Stokes signal from Fig. 5 as approximately 0.3 volts, we can compare the two intensities of the 8283Å line, one from the Raman Stokes signal, the other form the combustion spectrum. We find:

COMBUSTION SPECTRUM	RAMAN STOKES SIGNAL
8689 "counts" = 1.497721×10^6 photons	0.3 v. = 9.375×10^5 photons

So we see in this particular case the radiation from the combustion light at 8283Å is actually greater than the Stokes signal at 8283Å before combustion! We can actually expect a worse condition than this since the Stokes signal will decrease somewhat during combustion (a comparison of 5976Å [the anti-Stokes line] is not possible since the Raman anti-Stokes data could not be obtained during combustion and cannot be obtained in a cool gas). However, this situation creates a paradox. If the signal from the combustion spectrum would be greater than the Raman signal itself, why doesn't the phototube register an output voltage instead of zero? This question and the problem of the water vapor itself remain to be resolved.

Future Considerations

Here are some ways in which some problems may be overcome or different approaches used in this type of experiment:

1. Instead of monitoring nitrogen (N_2) to observe the temperature during the combustion, use water (H_2O) since water is also Raman active. There should be sufficient water vapor generated at the maximum heat release point to receive both water Raman lines.
2. Monitor nitrogen but use a light source other than the (6943Å) which preferably is not totally absorbed by water. Since green is a line not readily absorbed by water a doubled Nd yag laser might be a good choice. Further, a pulsed, high-repetition Nd yag laser would allow close interval monitoring of the evolution of the combustion temperature change and possibly the varying pressure and density associated with the propagating explosion shock front.
3. Analyze the temperature of the entire combustion directly by utilizing the monitoring of the entire radiation spectrum released during combustion. Find correlations between weak and strong com-

bustions and the intensity of the light radiation released. Relate the absence or presence of certain species to specific changes in the combustion spectrum profile. Obtain the light spectrums of several fuels and compare for similarities, if any.

Acknowledgement

This research was sponsored by the National Aeronautics and Space Administration under Grant NSG 3108.

References

Lederman, S.: The Use of Laser Raman Diagnostics in Flow Fields and Combustion. Progr. Energy Comb. Sci., Vol. 3, pp. 1-34, 1977, Perg. Press.

Lederman, S.: Laser Based Diagnostic Techniques for Combustion Research. AIAA Progress in Astronautics and Aeronautics, Vol. 58, pp. 291-309, 1968.

Lederman, S.: Modern Diagnostics of Combustion. Experimental Diagnostics in Gas Phase Combustion Systems, Vol. 53. Editor Ben T. Zinn.

Lederman, S., Bloom, M.H., Bornstein, J. & Khosla, P.K.: Temperature and Specie Concentration Measurements in a Flow Field. Int. J. Heat Mass Transfer, Vol. 17, 12, pp. 1479-1486, December 1974.

Lederman, S. & Bornstein, J.: Experimental Investigation of Coaxial Turbulent Jets. Israel J. of Technology, Vol. 14, pp. 241-249, 1976.

Lederman, S.: Experimental Techniques Applicable to Turbulent Flows. Presented at the AIAA 15th Aerospace Sciences Meeting, Los Angeles, CA., AIAA Paper No. 77-213, 1977.

Lederman, S., Celentano, A. and Glaser, J.: Temperature, Concentration and Velocity in Jets, Flames and Shock Tubes. Phys. of Fluids, Vol. 22, 6, p. 1065, June 1979.

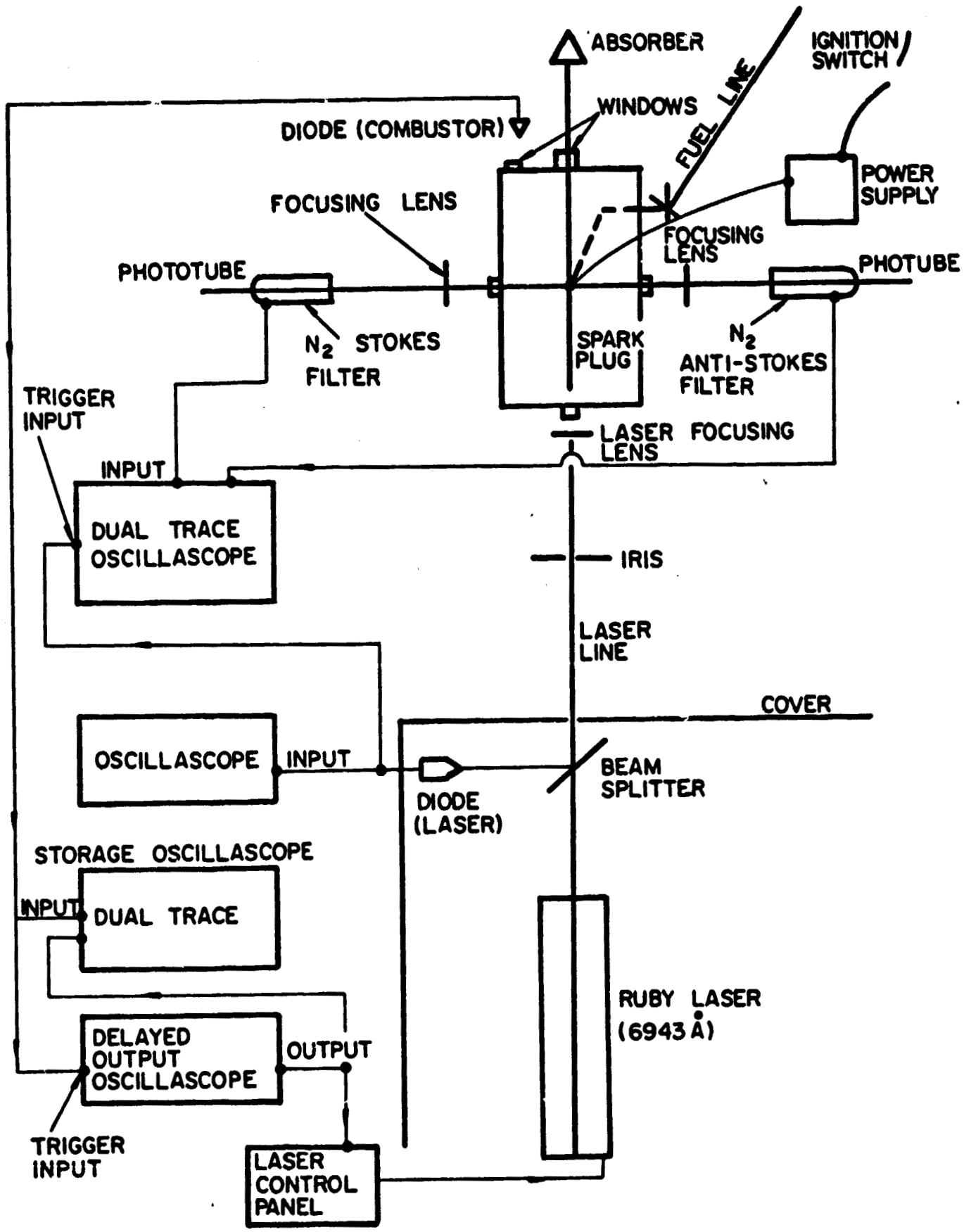

FIG. 1 SCHEMATIC SET-UP

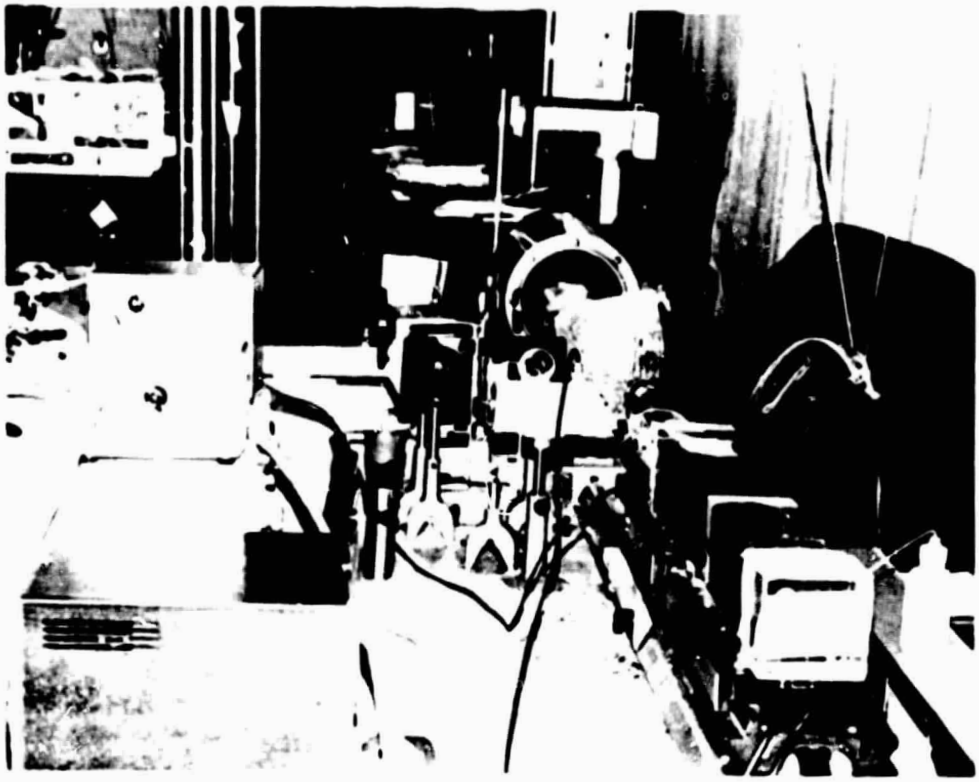

FIG. 2 PHOTOGRAPHIC VIEW OF THE EXPERIMENTAL APPARATUS

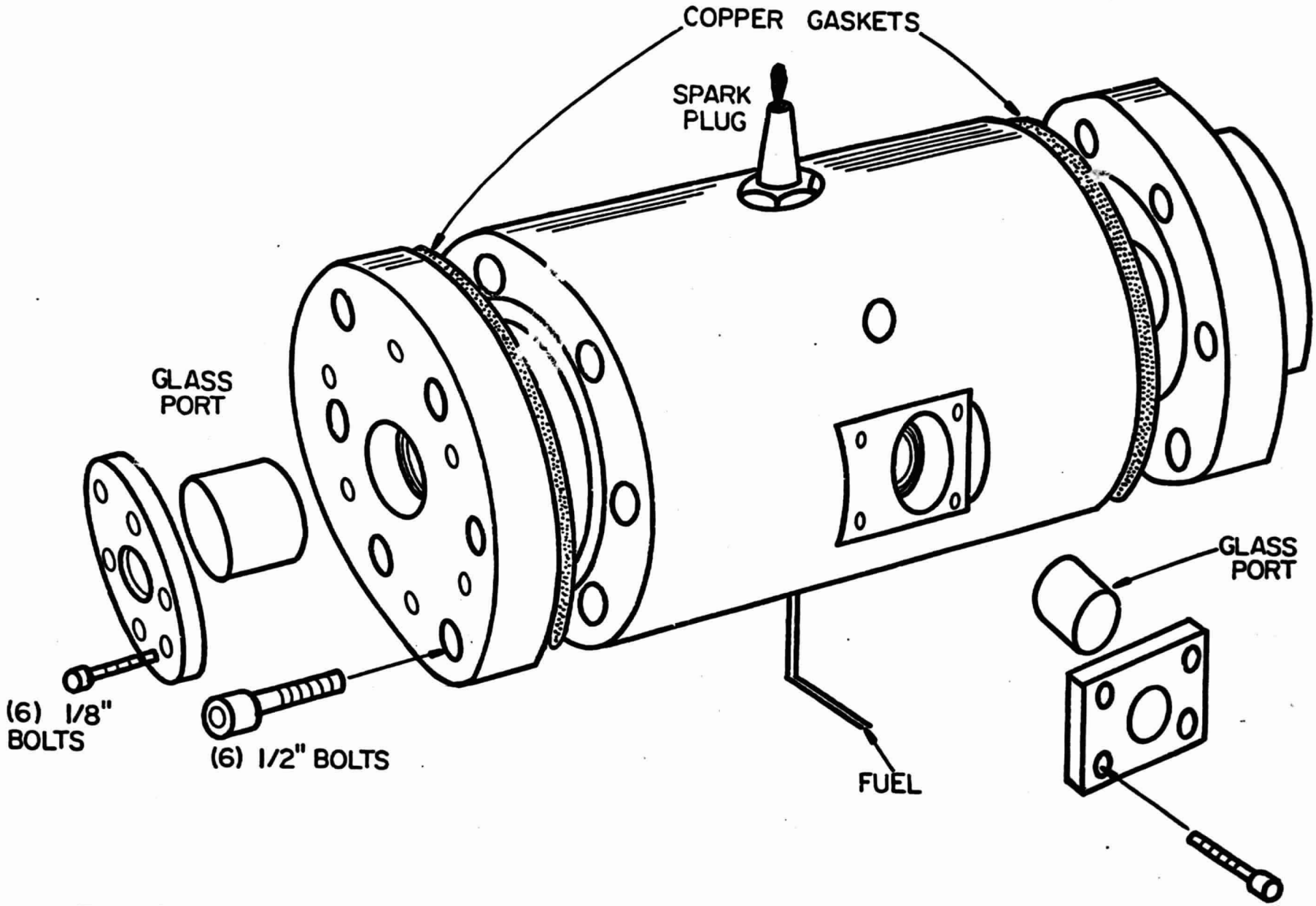

FIG. 3a COMBUSTION CHAMBER

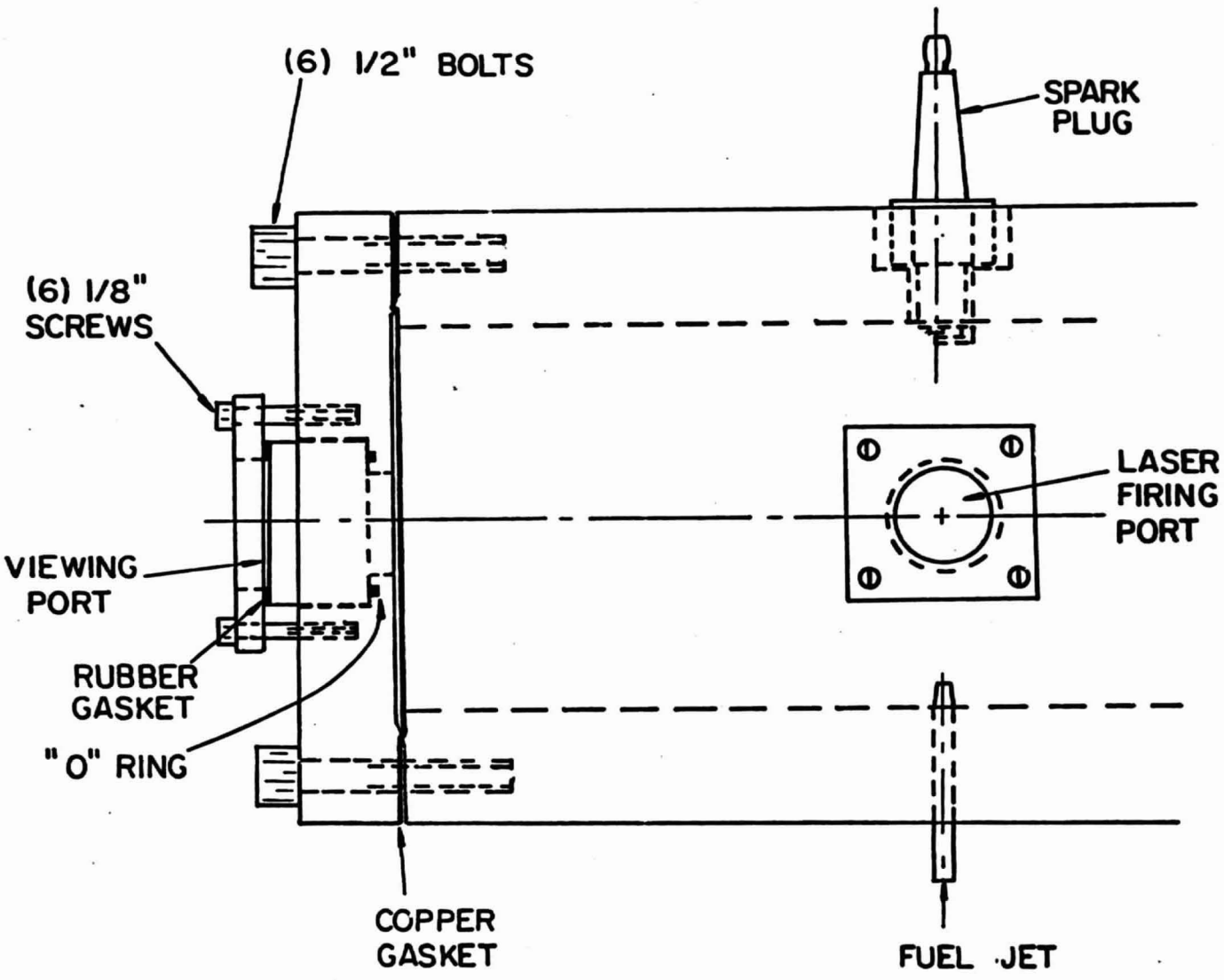

FIG. 3b COMBUSTION CHAMBER SKETCH

COMBUSTION
NO. 1

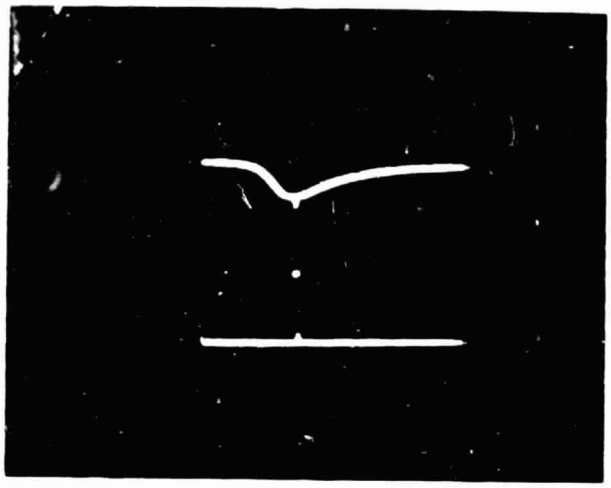

PHOTODIODE
1V/DIV

TRIGGER PULSE
5V/DIV
VARIOUS DELAYS

COMBUSTION
NO. 2

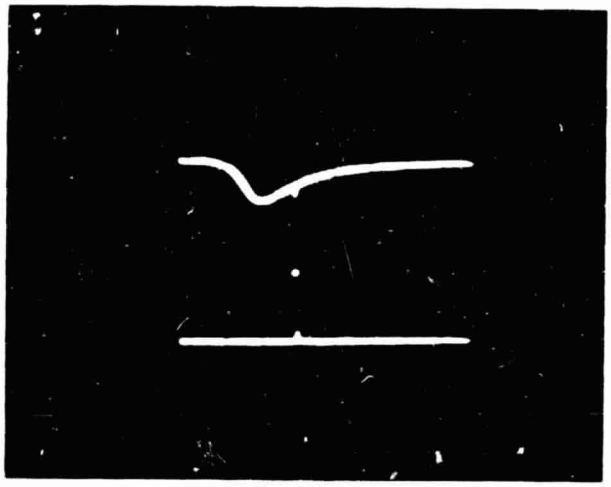

PHOTODIODE
1V/DIV

TRIGGER PULSE
5V/DIV
VARIOUS DELAYS

COMBUSTION
NO. 3

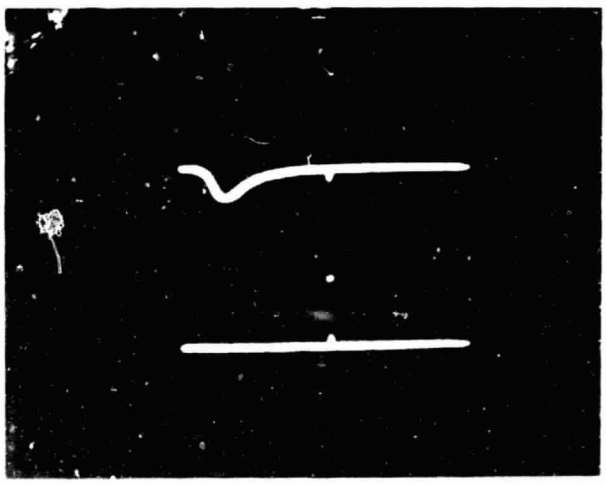

PHOTODIODE
1V/DIV

TRIGGER PULSE
5V/DIV
VARIOUS DELAYS

FIG. 4

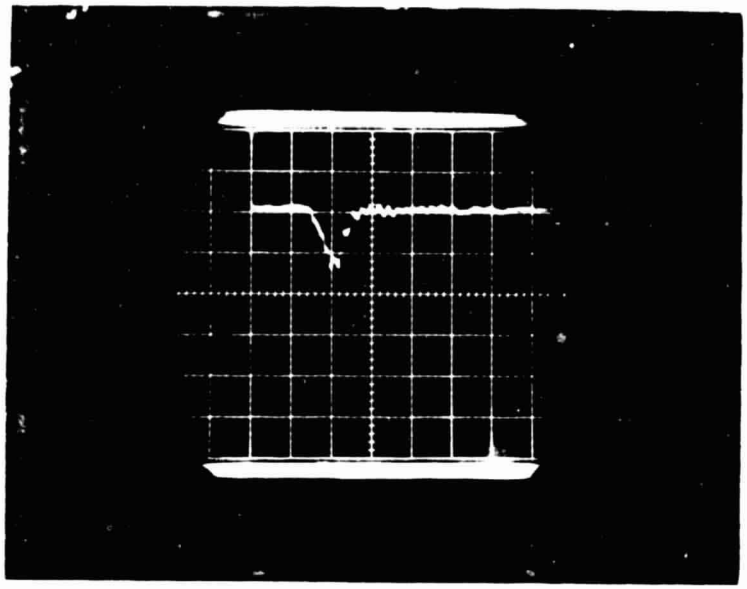

BACKROUND
VACUUM 0.4 TORR

50nsec SWEEP
0.1v/div

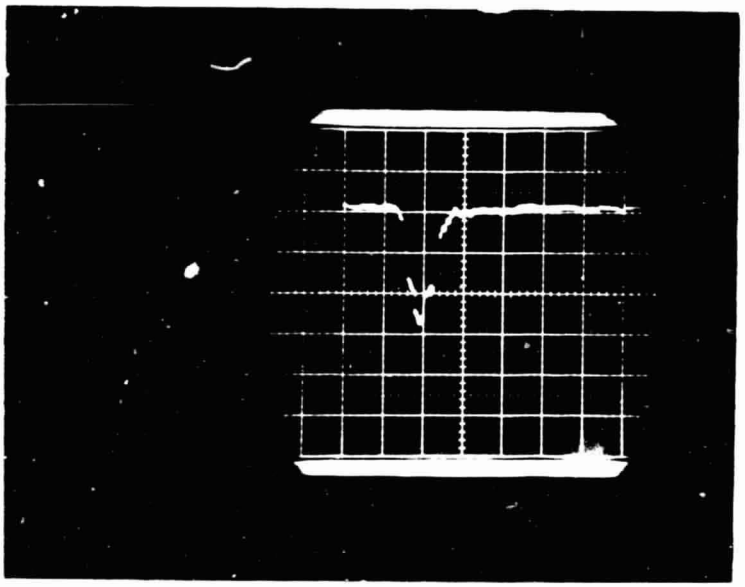

RAMAM STOKES N_2

FIG. 5

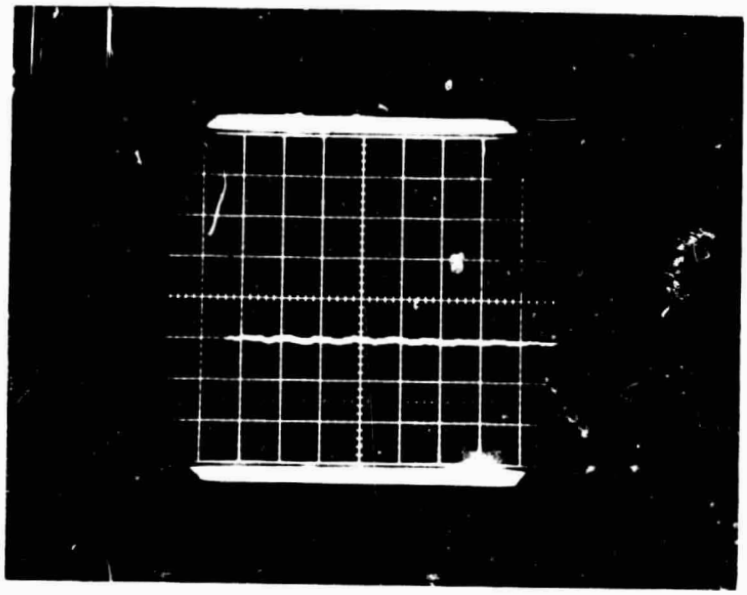

RAMAN STOKES N_2
50 nsec SWEEP
0.1 v/div

100 msec
DELAY

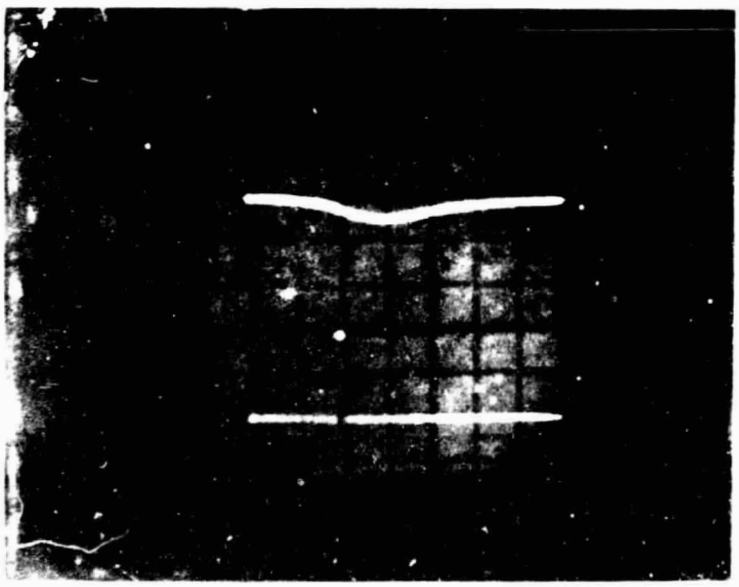

PHOTODIODE
1 v/div

TRIGGER PULSE
5 v/div

FIG. 6

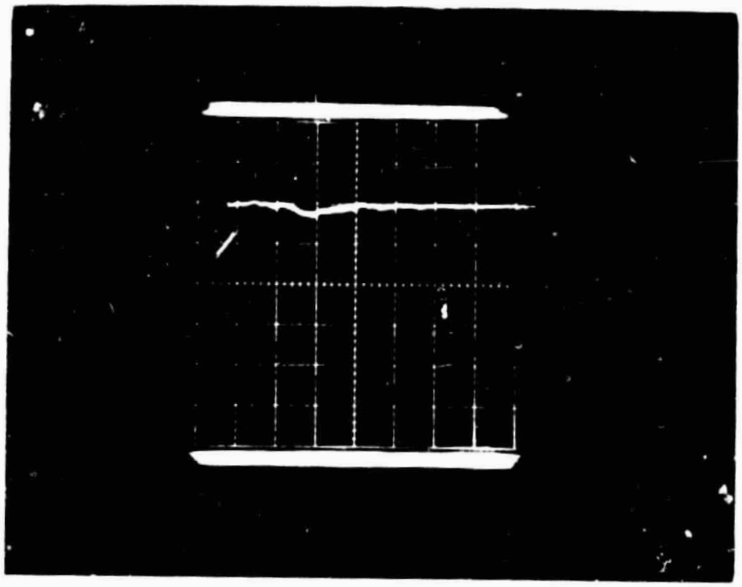

RAMAN STOKES N_2
50 nsec SWEEP
0.1v /div

300 msec DELAY

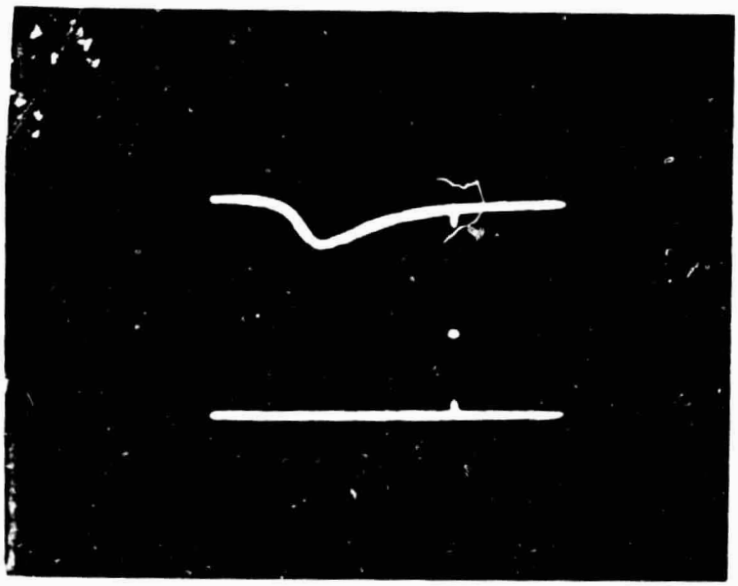

PHOTODIODE
1v/div

TRIGGER PULSE
5 v /div

FIG. 7

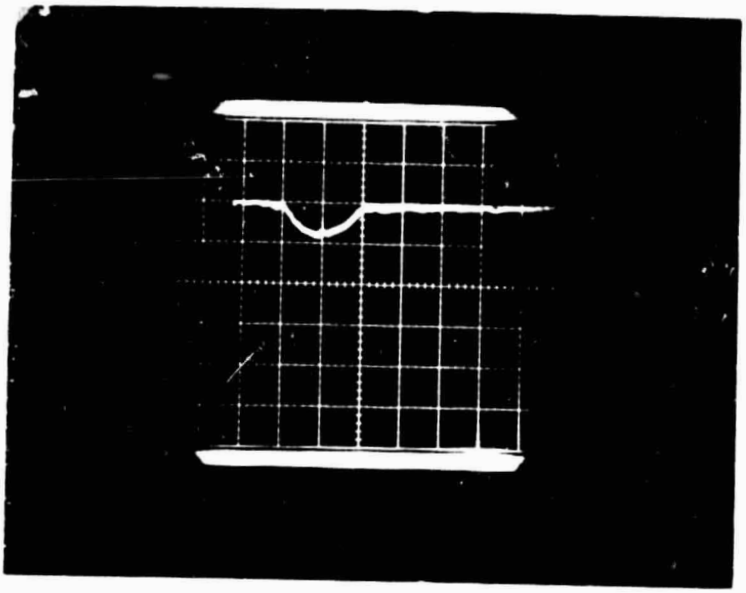

RAMAN STOKES N_2
50 n sec SWEEP
0.1 v / div

350 msec DELAY

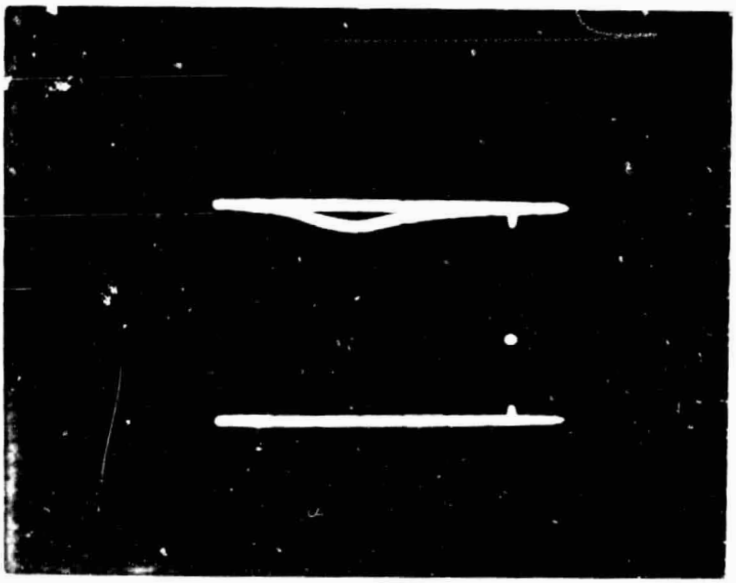

PHOTODIODE
1v / div

TRIGGER PULSE
5v / div

FIG. 8

30 sec
60 sec
90 sec AFTER
EXPLOSION

STOKES SIGNAL

120 sec
150 sec
180 sec AFTER
EXPLOSION

STOKES SIGNAL

FIG. 9

– 32768 FULL SCALE
– 150 SCANS
– 0.01028 sec/INTERVAL

HIGHEST PEAK: 7132 Å
COUNT: 21554

ALSO:
(STOKES, ANTI-STOKES: COUNT)

N_2	8283 : 8689 5976 : 10084	O_2	7783 : 11229 6266 : 10382
CO_2	7623 : 13241 6373 : 9920	CH_4	8704 : ---- 5774 : 9835
NO_2	7326 : 17758 6597 : 10493	H_2O	9301 : ---- 5538 : 10044

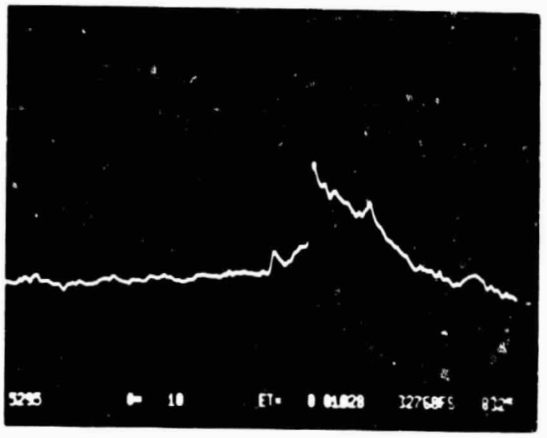

5295 Å - - - - - - - 8325 Å

BACKROUND

AVERAGE COUNT: 61

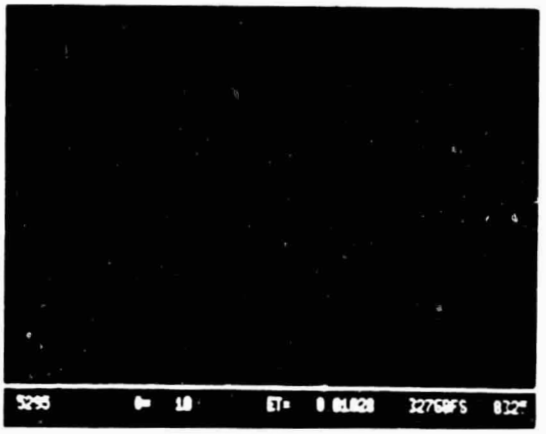

5295 Å - - - - - - - 8325 Å

REPEAT COMBUSTION SPECTRUM:
HIGHEST PEAK: 7132 Å

N_2	S : 7388 AS : 12098	O_2	S : 11618 AS : 12860
CO_2	S : 14535 AS : 11960	CH_4	S : --- AS : 11243
NO_2	S : 20237 AS : 12967	H_2O	S : --- AS : 11638

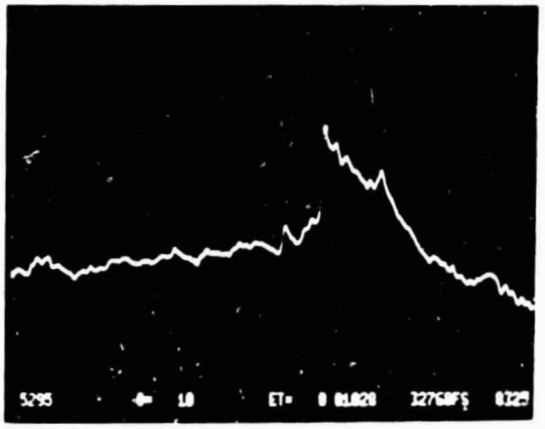

5295 Å - - - - - - - 8325 Å

FIG 10 COMBUSTION SPECTRUM (CH-AIR)
(ARRAY DETECTOR)